

Improved heat-spreading properties of fluorinated graphite/epoxy film

Kyung Hoon Kim, Jeong-In Han, Da-Hee Kang, and Young-Seak Lee^{*}

Department of Chemical Engineering and Applied Chemistry, Chungnam National University, Daejeon 34134, Korea

Article Info

Received 12 March 2018

Accepted 27 March 2018

*Corresponding Author

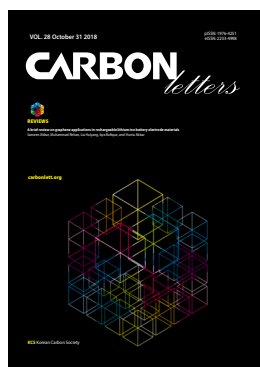
E-mail: youngslee@cnu.ac.kr

Tel: +82-42-821-7007

Open Access

DOI: <http://dx.doi.org/10.5714/CL.2018.28.096>

This is an Open Access article distributed under the terms of the Creative Commons Attribution Non-Commercial License (<http://creativecommons.org/licenses/by-nc/3.0/>) which permits unrestricted non-commercial use, distribution, and reproduction in any medium, provided the original work is properly cited.



<http://carbonlett.org>

pISSN: 1976-4251

eISSN: 2233-4998

Copyright © Korean Carbon Society

The use of electronic devices has rapidly increased, and such devices are required to be smaller, thinner, lighter, and with higher energy densities than ever before. These requirements can result in the generation of additional heat during device operation, and this heat has detrimental effects on performance, stability, running rate, and lifespan. For instance, if the temperature of an electronic device increases by 2°C when the operating temperature is higher than the stable operating temperature, the stability of the device will be reduced by 10% [1-3]. Thus, the additional heat that such devices generate must be spread to the surrounding environment via heat sinks, coatings, or films with high thermal conductivity.

The use of coatings and films is an appropriate approach for improving the heat spread in electronic devices, particularly as these devices become lighter, smaller, and thinner. Such coatings and films are typically based on polymers such as epoxy, acryl, and polyurethane. Due to the low thermal conductivity of these polymers, it is difficult to use this approach to achieve effective heat spreading. To solve this problem, a great deal of research has addressed the addition of fillers with high thermal conductivity, such as aluminum nitride [4,5], silica (SiO₂), alumina (Al₂O₃), boron nitride [1,6,7], graphite [8], expanded graphite (EG) [9-11], carbon nanotubes (CNTs) [11-13], graphene [9,14,15], and graphene oxide (GO) to polymer-based coatings. Recently, carbon-based materials such as graphite, EG, CNTs, graphene, and GO have been widely investigated because of their low density and high thermal conductivity. However, CNTs and graphene are not appropriate for large-scale applications due to their high production cost and complex processing. In addition, fillers with poor dispersive stability aggregate in coatings form voids, resulting in the degradation of thermal conductivity [16,17]. In this study, anionic fluorine functional groups are introduced into a graphite surface via direct fluorination to increase dispersive stability by generating electrostatic repulsion. We expect the enhanced dispersive stability of the modified graphite to lead to the formation of fewer voids, resulting in improved thermal conductivity of the prepared heat-spreading film.

Diglycidyl ether of bisphenol A (DGEBA; YD-128, Kukdo Chemical Co., Korea) with a viscosity of 11,500 to 13,500 cP was used as the epoxy monomer, and polyamide resin (G-640, Kukdo Chemical Co.) with a viscosity of 8,000 to 12,000 cP was used as the curing agent for the epoxy resin. Acetone was used as a diluent for the epoxy resin. Fluorine gas (99.8%, Messer Griesheim GmbH, Germany) was used to introduce anionic fluorine functional groups into the graphite surface. The following fluorination method was used for this introduction. Graphite was loaded into a nickel boat and placed into a batch reactor. Degassing was performed for 1 h at room temperature using a vacuum pump. Subsequently, a mixture of fluorine gas and nitrogen gas (at a partial pressure ratio of F₂:N₂=1:9) at a total pressure of 1 bar was placed into the reactor, and fluorination was conducted for 10 min at room temperature. Pristine graphite and fluorinated graphite were labeled PG and FG, respectively. Filler-free coatings were prepared by mixing the epoxy resin, polyamide resin, and acetone (2:1:2 by wt%) using a planetary mixer at 2000 rpm for 1 min. Filler (PG or FG) was added (at a wt% of 10%) to the prepared coatings by continuous mixing at 2000 rpm for 5 min, and the coatings were sonicated in an ultrasonic bath for 10 min to achieve uniform dispersion. A copper plate was coated with the prepared coatings with a wet thickness of 250 μm, and then cured in an oven at 100°C for 30 min. To investigate the functional groups introduced into the surface of the PG and FG, X-ray photoelectron spectroscopy (XPS; Mul-

tiLab 2000, Thermo Electron Co., UK) analysis was performed using Al K α radiation (1485.6 eV), and a peak analysis program was utilized to deconvolute the C1s peaks using the pseudo-Voigt function. X-ray diffraction (XRD) and Raman spectroscopy were conducted to investigate differences in the structures of PG and FG [18]. XRD patterns generated using Cu K α radiation were recorded using an X'Pert PRO multipurpose X-ray diffractometer (PANalytical, the Netherlands). Raman scattering spectra were obtained using a micro-Raman spectrometer (NRS-5100, JASCO) and an excitation source with a 532 nm CW laser. UV-Vis spectrometry (Optizen 2120 UV, Mecasys, Korea) was used to investigate the dispersion of PG and FG in the tested coatings. In this analysis, the coatings were diluted to allow for detailed evaluation of the effects of the introduced fluorine functional groups on dispersion. In particular, for this assessment, the coatings were prepared using an epoxy resin:polyamide resin:acetone ratio of 2:1:7 (by wt%), and 0.1 wt% prepared graphite was then added to the diluted coatings. After samples were sonicated for 10 min, transmittance was measured at a wavelength of 700 nm for 10 h. The morphology of the prepared coatings was examined using field-emission scanning electron microscopy (FE-SEM; JSM-7500, Hitachi, Japan) to investigate the dispersion status of the graphite. The thermal conductivities of the prepared samples were measured at 50 to 250°C using laser flash method (LFA 447, NETZSCH, Germany).

The effects of direct fluorination on the surface composition and chemical bonds of graphite were investigated using XPS. Fig. 1 shows XPS survey spectra and elemental analysis results. As shown in Fig. 1a, fluorine, oxygen, and carbon peaks were observed at binding energies of 684–694, 528–538, and 282–294 eV, respectively. Only carbon and oxygen peaks were present for PG, whereas a fluorine peak was detected on the surface of FG. In particular, in FG, fluorine was introduced at 12.46 at% after direct fluorination.

To investigate the introduced fluorine functional groups in detail, FG was analyzed via F1s deconvolution using the pseudo-Voigt function and a peak analysis program. The deconvoluted results for the F1s spectra for FG indicate that covalent and semi-covalent C–F bonds were observed at binding energies of 688.5 and 686.8 eV, respectively [19–21]. The concentrations of covalent and semi-covalent C–F bonds on the surface of FG were 9.8% and 90.2%, respectively. The FG surface has anionic properties because of the large electronegativity difference between carbon and fluorine. The fluorination-induced changes in the chemical composition on the surface of FG can generate electrostatic repulsion between each particle due to the surface negative charge of the introduced C–F bonds.

In addition, to investigate structural changes in the prepared graphite after direct fluorination, the D_{002} spacing and I_D/I_G values of the prepared graphite were evaluated using XRD and Raman spectroscopy, respectively. PG and FG had D_{002} spacing of 3.389 and 3.385, respectively, and I_D/I_G values of 2.34 and 2.27, respectively. Fluorine functional groups were introduced into the graphite surface, as described above, but no large structural changes were observed. In fact, for PG and FG, D_{002} spacing differed by less than 0.12%, and I_D/I_G differed by less than 3%. Therefore, direct fluorination can introduce anionic fluorine functional groups into the graphite surface with few structural changes.

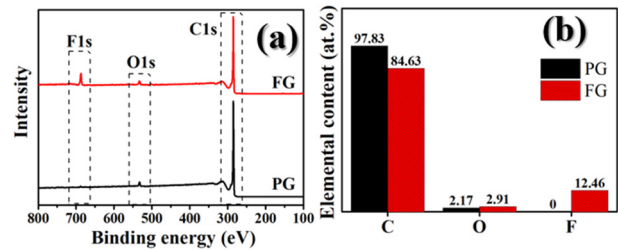


Fig. 1. XPS survey spectra for PG and FG (a) and elemental content on the surface of PG and FG (b).

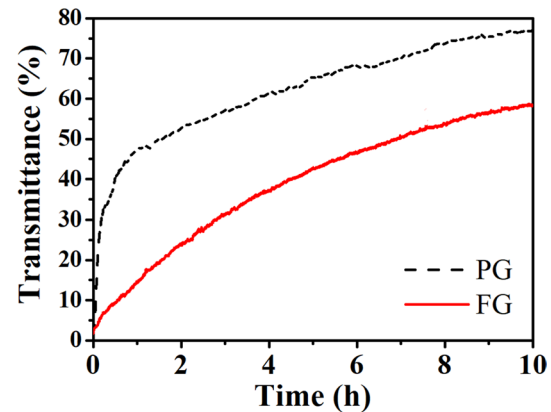


Fig. 2. UV-Vis transmittance spectra for PG and FG in diluted epoxy-based coatings.

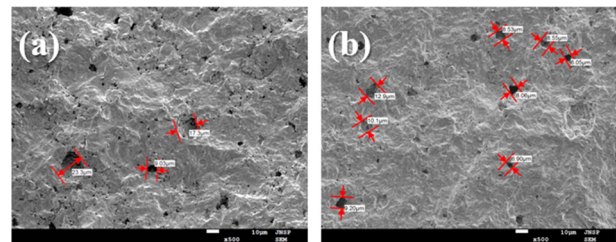


Fig. 3. SEM images of PG-based film (a) and FG-based film (b).

The dispersive stability of the filler in coatings is an extremely important factor in the preparation of uniform coatings in which filler particles do not aggregate. To enhance the thermal conductivity of coatings via the addition of a thermally conductive filler such as graphite, which is used in this research, the aggregation of filler particles must be reduced because such aggregation results in the formation of voids in coatings after curing; the presence of such voids is known to lead to extremely low thermal conductivity. Thus, to investigate dispersive stability, the prepared graphite in coatings diluted with acetone was evaluated using UV-Vis spectrophotometry at a wavelength of 700 nm, as shown in Fig. 2 [22,23]. From the start of measurement to 10 h, the transmittances of PG and FG increased to 76.8% and 58.2%, respectively. The rate of sedimentation was higher for FG than for PG at the initial time point, as indicated by the initial slope of the graph. This phenomenon is attributable to improved dis-

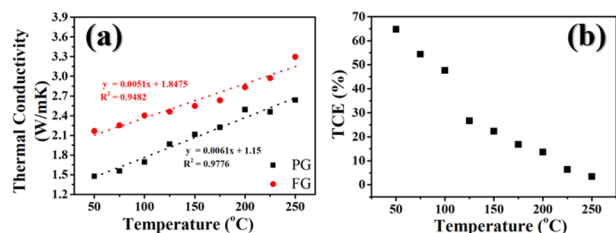


Fig. 4. Thermal conductivities of prepared films (a) and the corresponding values for TCE (b).

persive stability of FG due to electrostatic repulsion between FG particles induced by the anionic C–F bonds introduced via direct fluorination.

Thermal conductivities of the prepared films were obtained using laser flash method at 50 to 25°C, and the experimental results are shown in Fig. 4a. These thermal conductivities increased as the measured temperature increased. Thermal conductivity was higher for the FG-based film than for the PG-based film. Thermal conductivity enhancement (TCE) for the FG-based film compared with the PG-based film was calculated by Eq 1, and the results are shown in Fig. 4b [24].

$$\text{TCE}(\%) = \frac{(TC_{FG} - TC_{PG})}{TC_{PG}} \times 100 \quad (1)$$

TCE was positive at all temperatures tested in this study but decreased as the temperature increased. In particular, at 50°C, the thermal conductivity of the FG-based film was approximately 65% greater than that of the PG-based film.

In conclusion, heat-spreading film with directly fluorinated graphite added as filler was prepared to investigate the effects of direct fluorination of the graphite surface on dispersive stability and thermal conductivity. The addition of fluorine functional groups to the graphite surface effectively enhanced dispersive stability by generating electrostatic repulsion. This alteration reduced the agglomeration of graphite particles, leading to decreases in the number of voids and void size in coatings, and thereby resulting in increased thermal conductivity. Thus, direct fluorination of graphite surfaces can improve the dispersive stability and thermal conductivity of heat-spreading film.

Conflict of Interest

No potential conflict of interest relevant to this article was reported.

Acknowledgements

This work is partially supported by the Korea Institute of Energy Technology Evaluation and Planning (KETEP) grant funded by the Ministry of Trade, Industry & Energy (MOTIE) of the Republic of Korea (No. 20164010201070), and is also one of the results of a study on the “Leaders in Industryuniversity Cooperation +” project, supported by the Ministry of Education and the National Research Foundation of the Republic of Korea.

References

- [1] Kim K, Kim M, Hwang Y, Kim J. Chemically modified boron nitride-epoxy terminated dimethylsiloxane composite for improving the thermal conductivity. *Ceram Int*, **40**, 2047 (2014). <https://doi.org/10.1016/j.ceramint.2013.07.117>.
- [2] Kim JH, Kim KH, Park MS, Bae TS, Lee YS. Cu nanoparticle-embedded carbon foams with improved compressive strength and thermal conductivity. *Carbon Lett*, **17**, 65 (2016). <https://doi.org/10.5714/cl.2016.17.1.065>.
- [3] Han Z, Fina A. Thermal conductivity of carbon nanotubes and their polymer nanocomposites: a review. *Prog Polym Sci*, **36**, 914 (2011). <https://doi.org/10.1016/j.progpolymsci.2010.11.004>.
- [4] Kim K, Kim J. Magnetic aligned AlN/epoxy composite for thermal conductivity enhancement at low filler content. *Compos Part B Eng*, **93**, 67 (2016). <https://doi.org/10.1016/j.compositesb.2016.02.052>.
- [5] Yuan W, Xiao Q, Li L, Xu T. Thermal conductivity of epoxy adhesive enhanced by hybrid graphene oxide/AlN particles. *Appl Therm Eng*, **106**, 1067 (2016). <https://doi.org/10.1016/j.applthermaleng.2016.06.089>.
- [6] Donnay M, Tzavalas S, Logakis E. Boron nitride filled epoxy with improved thermal conductivity and dielectric breakdown strength. *Compos Sci Technol*, **110**, 152 (2015). <https://doi.org/10.1016/j.compscitech.2015.02.006>.
- [7] Yu C, Zhang J, Li Z, Tian W, Wang L, Luo J, Li Q, Fan X, Yao Y. Enhanced through-plane thermal conductivity of boron nitride/epoxy composites. *Compos Part A Appl Sci Manuf*, **98**, 25 (2017). <https://doi.org/10.1016/j.compositesa.2017.03.012>.
- [8] Yu A, Ramesh P, Itkis ME, Bekyarova E, Haddon RC. Graphite nanoplatelet: epoxy composite thermal interface materials. *J Phys Chem C*, **111**, 7565 (2007). <https://doi.org/10.1021/jp071761s>.
- [9] Balandin AA, Ghosh S, Bao W, Calizo I, Teweldebrhan D, Miao F, Lau CN. Superior thermal conductivity of single-layer graphene. *Nano Lett*, **8**, 902 (2008). <https://doi.org/10.1021/nl0731872>.
- [10] Wang Z, Qi R, Wang J, Qi S. Thermal conductivity improvement of epoxy composite filled with expanded graphite. *Ceram Int*, **41**, 13541 (2015). <https://doi.org/10.1016/j.ceramint.2015.07.148>.
- [11] Shou QL, Cheng JP, Fang JH, Lu FH, Zhao JJ, Tao XY, Liu F, Zhang XB. Thermal conductivity of poly(vinylidene fluoride) composites filled with expanded graphite and carbon nanotubes. *J Appl Polym Sci*, **127**, 1697 (2013). <https://doi.org/10.1002/app.37876>.
- [12] Chu K, Jia C, Li W. Thermal conductivity enhancement in carbon nanotube/Cu–Ti composites. *Appl Phys A*, **110**, 269 (2013). <https://doi.org/10.1007/s00339-012-7450-0>.
- [13] Che J, Çagin T, Goddard WA III. Thermal conductivity of carbon nanotubes. *Nanotechnology*, **11**, 65 (2000). <https://doi.org/10.1088/0957-4484/11/2/305>.
- [14] Wang F, Drzal LT, Qin Y, Huang Z. Mechanical properties and thermal conductivity of graphene nanoplatelet/epoxy composites. *J Mater Sci*, **50**, 1082 (2015). <https://doi.org/10.1007/s10853-014-8665-6>.
- [15] Shahil KMF, Balandin AA. Thermal properties of graphene and multilayer graphene: Applications in thermal interface materials. *Solid State Commun*, **152**, 1331 (2012). <https://doi.org/10.1016/j.ssc.2012.04.034>.
- [16] Nika DL, Pokatilov EP, Askerov AS, Balandin AA. Phonon thermal conduction in graphene: role of Umklapp and edge roughness scattering. *Phys Rev B*, **79**, 155413 (2009). <https://doi.org/10.1103/physrevb.79.155413>.

- [17] Raunija TSK, Supriya N. Thermo-electrical properties of randomly oriented carbon/carbon composite. *Carbon Lett*, **22**, 25 (2017). <https://doi.org/10.5714/CL.2017.22.025>.
- [18] Kim JH, Lee HI, Lee YS. The enhanced thermal and mechanical properties of graphite foams with a higher crystallinity and apparent density. *Mater Sci Eng A*, **696**, 174 (2017). <https://doi.org/10.1016/j.msea.2017.04.071>.
- [19] Lee C, Han YJ, Seo YD, Nakabayashi K, Miyawaki J, Santamaría R, Menéndez R, Yoon SH, Jang J. C_4F_8 plasma treatment as an effective route for improving rate performance of natural/synthetic graphite anodes in lithium ion batteries. *Carbon*, **103**, 28 (2016). <https://doi.org/10.1016/j.carbon.2016.02.060>.
- [20] Lee YS. Syntheses and properties of fluorinated carbon materials. *J Fluorine Chem*, **128**, 392 (2007). <https://doi.org/10.1016/j.jfluchem.2006.11.014>.
- [21] Yun SM, Kim JW, Jung MJ, Nho YC, Kang PH, Lee YS. An XPS study of oxyfluorinated multiwalled carbon nano tubes. *Carbon Lett*, **8**, 292 (2007). <https://doi.org/10.5714/cl.2007.8.4.292>.
- [22] Im JS, Kim JG, Lee SH, Lee YS. Enhanced adhesion and dispersion of carbon nanotube in PANI/PEO electrospun fibers for shielding effectiveness of electromagnetic interference. *Colloids Surf A Physicochem Eng Aspects*, **364**, 151 (2010). <https://doi.org/10.1016/j.colsurfa.2010.05.015>.
- [23] Im JS, Kim JG, Lee YS. Fluorination effects of carbon black additives for electrical properties and EMI shielding efficiency by improved dispersion and adhesion. *Carbon*, **47**, 2640 (2009). <https://doi.org/10.1016/j.carbon.2009.05.017>.
- [24] Kim C, Baek JY, Kim DH, Kim JT, Lopez DH, Kim T, Kim H. Decoupling of thermal and electrical conductivities by adjusting the anisotropic nature in tungsten diselenide causing significant enhancement in thermoelectric performance. *J Ind Eng Chem*, **60**, 458 (2018). <https://doi.org/10.1016/j.jiec.2017.11.033>.